[redacted]

NASA TECHNICAL MEMORANDUM

UB
NASA TM X-1389

[redacted]

SPECTRAL MEASUREMENTS OF GAS-CAP RADIATION DURING PROJECT FIRE FLIGHT EXPERIMENTS AT REENTRY VELOCITIES NEAR 11.4 KILOMETERS PER SECOND

by Dona L. Cauchon, Charles W. McKee, and Elden S. Cornette

Langley Research Center
Langley Station, Hampton, Va.

NATIONAL AERONAUTICS AND SPACE ADMINISTRATION • WASHINGTON, D. C. • OCTOBER 1967

[redacted]

[redacted]

NASA TM X-1389

SPECTRAL MEASUREMENTS OF GAS-CAP RADIATION DURING PROJECT FIRE FLIGHT EXPERIMENTS AT REENTRY VELOCITIES NEAR 11.4 KILOMETERS PER SECOND

By Dona L. Cauchon, Charles W. McKee, and Elden S. Cornette

Langley Research Center
Langley Station, Hampton, Va.

[redacted]

Technical Film Supplement L-961, Parts I and II, available on request.

[redacted]

[redacted]

[redacted]

NATIONAL AERONAUTICS AND SPACE ADMINISTRATION

[redacted]

U. S. Government Agencies and
ontractors Only

SPECTRAL MEASUREMENTS OF GAS-CAP RADIATION DURING PROJECT FIRE FLIGHT EXPERIMENTS AT REENTRY VELOCITIES NEAR 11.4 KILOMETERS PER SECOND*

By Dona L. Cauchon, Charles W. McKee,
and Elden S. Cornette
Langley Research Center

SUMMARY

Selected spectral distributions of radiation intensity obtained during the Project Fire reentries have been evaluated and compared with existing theories. Near peak heating the spectra, which cover a nominal wavelength range from 0.2μ to 0.6μ, corroborate with fair accuracy most theoretical preflight predictions of equilibrium radiation. The results of the nonequilibrium radiation measurements obtained early in the reentry were orders of magnitude smaller than preflight predictions.

INTRODUCTION

The primary objective of Project Fire was to determine the radiative and total heating to a large-scale, blunt, Apollo-shaped vehicle entering the earth atmosphere at a velocity of approximately 11.4 kilometers per second (37 000 feet per second). The program provided for two flights launched from Cape Kennedy, Florida, down the Eastern Test Range with reentries in the vicinity of Ascension Island. In addition to obtaining calorimeter and broadband radiometer measurements ($\lambda > 0.2\mu$) (refs. 1 to 4), the Fire experiments provided measurements of spectral distributions of the stagnation radiation over the 0.2μ to 0.6μ wavelength range. The intent of this report is to present selected Fire spectra in this range. Comparisons with preflight estimates were also made.

Film-strip supplements (film serial L-961, Parts I and II) have been prepared and are available on loan. A request card form and a description of the film strip will be found at the back of this report. A discussion of the supplemental data is presented in the appendix.

[redacted]

SYMBOLS

N^+	ionized atomic nitrogen
$N_2^+(1-)$	ionized molecular nitrogen – first negative system
O^+, O^-	ionized atomic oxygen
p	pressure, newtons per meter^2 (pounds force per foot^2)
T	temperature, ^oK
t	time, seconds
V	velocity, kilometers per second (feet per second)
λ	wavelength, microns ($1\mu = 10^{-6}$ meters)
$\Delta\lambda$	wavelength interval, microns
ρ	density, kilograms per meter^3 (pounds mass per foot^3)

Subscripts:

ref	reference conditions ($T_{ref} = 273.15^o$ K (491^o R); $\rho_{ref} = 1.295$ kg/m^3 (8.073×10^{-2} lbm/ft^3); $p_{ref} = 1.011 \times 10^5$ N/m^2 (2117.69 lbf/ft^2))
std	sea-level conditions for 1962 U.S. Standard Atmosphere ($T_{std} = 288.15^o$ K (518.67^o R); $\rho_{std} = 1.225$ kg/m^3 (7.647×10^{-2} lbm/ft^3); $p_{std} = 1.010 \times 10^5$ N/m^2 (2116.22 lbf/ft^2)
∞	free-stream conditions for flight
I	Project Fire flight I
II	Project Fire flight II
2	equilibrium condition behind shock

[redacted]

[redacted]

EXPERIMENT DESIGN

Objectives

In addition to providing for the broadband measurement of radiation from the plasma in the stagnation region of the reentry package flow field, the Project Fire experiment was designed to obtain spectral distributions of this radiation in the 0.2μ to 0.6μ wavelength range. The choice of this particular range for obtaining narrowband spectral measurements was based upon the theoretical estimates of hot air radiation (refs. 5, 6, and 7) that prevailed at the time of the design of the experiment. The theory at that time indicated that during the course of the Fire reentry the radiation in the stagnation region would be dominated by molecular and continuum radiation in this 0.2μ to 0.6μ wavelength range. From these measurements it was expected that theoretical spectral distributions and the predicted influence of the various radiating species could be checked over a range of high-velocity flight conditions not accessible to ground facilities.

Data Period Concept

In order to obtain valid radiation measurements from the shocked air in the stagnation region, it was necessary to maintain a clean uncontaminated environment over the forebody of the Fire reentry package. A metallic calorimetric material not only allowed for the desired total heating measurements (from the combined radiative and convective modes) but also provided this clean environment. However, because no known calorimeter material could survive the complete reentry, the reentry package was designed with a layered forebody consisting of interspersed beryllium layers and phenolic-asbestos heat shields. The beryllium layers were used as calorimeters. The useful lifetime of these beryllium calorimeters served to define the prime experimental periods during which calorimetric and radiometric measurements were obtained. These three data periods provided for experiments during the early reentry, near peak heating, and at the lower velocities where the radiative heating was substantially reduced. Fused quartz optical windows installed in each of the forebody layers permitted concurrent direct measurement of the incident radiation from the forebody shock layer up to the time of window melting. Flight hardware and systems are discussed in detail in references 3, 4, and 8.

Instrumentation

Spectral radiometer design.- The Project Fire spectral radiometer was designed to measure the spectral distribution of radiation intensity of the shock-heated air in the stagnation flow field over the 0.2μ to 0.6μ wavelength range. This instrument consisted of a rocking diffraction grating as the primary dispersing element, the motion of which

alternately traversed the appointed spectrum of the gas cap in back and forth directions on successive scans. A prism served to divert the overlapping second order. A photomultiplier was used as the sensing element. This detector through its amplifier and associated circuitry provided a signal output to the prescribed telemetry link for ground readout. Provision was made for in-flight monitoring of the zero and full-scale reference levels as well as checking the intensity calibration signal from an internal source. A continuously illuminated internal mercury vapor lamp was included in the system to provide a scan time-wavelength calibration at low intensity levels. The spectral radiometer was housed in the same package as the stagnation total radiometer and shared some of the acceptance optics with that instrument. The radiometers viewed the radiating gas through fused quartz windows positioned in the various layers of the forebody structure. The acceptance cone for the stagnation radiometer had an included apex angle of about 8^{o} which remained well within the diameter of the windows. The transmissive quality of the quartz windows is included in reference 3. A more detailed description of the spectral radiometer design and calibration is included in reference 8.

Operational behavior of the flight instruments.- Continuous radiation measurements were obtained throughout the reentry. During ground-based data reduction, these analog data were digitized to provide a sampling rate of 10 000 samples/sec. This resulted in readings at 0.0004μ (4 Å) intervals, which provided approximately 1000 readings per instrument scan of the wavelength range from 0.2μ to 0.6μ. Approximately 300 radiometer scans were obtained during the heating portion of the Fire II reentry. However, only selected scans obtained during the clean calorimeter experimental periods are discussed in this report.

The radiometer bandpass was approximately 0.002μ (20 Å). However, the degradation of signal through the instrument and system electronics resulted in an overall spectral resolution for the radiometer of 0.004μ (40 Å). The scan time for one direction, excluding all reference level checks, was about 0.075 sec. The spectral radiometer exhibited about three decades of dynamic response (0.1 to 100 $W/cm^2\text{-sr-}\mu$) without instrument saturation.

Because of alinement difficulties in the Fire II instrument (resulting primarily from a prism tracking error which cut off the ultraviolet wavelengths), the spectral radiometer analysis was limited to the following spectral ranges:

Forward scan, 0.3000μ to 0.5575μ
Backward scan, 0.6090μ to 0.3000μ

A similar but less severe situation in the Fire I instrument resulted in the following wavelength coverage:

Forward scan, 0.2020μ to 0.5881μ
Backward scan, 0.5920μ to 0.2175μ

The relatively wide 0.004μ resolution of the spectral radiometer contributed to one particular deficiency in the measured spectra. That is, the intensity in a narrow line or band ($\Delta\lambda < 0.004\mu$) tends to be underestimated by the underfilling of the instrument bandpass.

Finally, the failure of the mercury-vapor calibration lamp to operate properly during either flight did not allow for any in-flight checking of the scan time-wavelength laboratory calibration. This shortcoming precluded any conclusive explanation of apparent shifts in the wavelength scales in the resulting spectra. The scan time-wavelength calibration curve in the final analysis was approximated by a straight line over the entire wavelength range from 0.2μ to 0.6μ for both scan directions. This method, although providing a reasonable fairing through a series of preflight calibration points obtained with a mercury-arc lamp, did presume perfect linearity of the mechanically driven apparatus.

An estimate of the accuracy of the intensities indicated by the spectral radiometer has been made for both the Fire I and Fire II experiments. This estimate has been presented in reference 6 in the form of root-sum-square (rss) deviations from the measured data. The resulting rss deviations are as follows:

First data period	±23 percent
Second data period	+24 percent
	-23 percent
Third data period	+25 percent
	-23 percent

The deviations are applicable to the broadband (0.004μ resolution) Fire data shown in figures 1 to 6.

RESULTS AND DISCUSSIONS

The spectral distributions of air radiation over the range of thermodynamic conditions exhibited in the stagnation flow field of the Fire reentry package have been discussed in many reports (e.g., refs. 5, 6, 7, 9, 10, and 11). Specific estimates of the spectral distribution of the intensity in the stagnation flow field for typical Fire reentry conditions have also been presented in references 12, 13, and 14. The analyses of the total radiometer data from the Fire II experiment coupled with the integrations of the spectral scans at the corresponding times indicated that about three-quarters of the radiation at $0.2\mu < \lambda < 4.0\mu$ occurred at $\lambda > 0.6\mu$. The ranges of stagnation equilibrium flow conditions during the first two data periods were $10\,400^{\circ}\text{ K} < T_2 < 11\,600^{\circ}\text{ K}$

and $5 \times 10^{-4} < \frac{\rho_2}{\rho_{ref}} < 10^{-2}$. In the third data period experiment, which was characterized by less severe flow conditions $\left(7500^{\circ}\ K < T_2 < 8000^{\circ}\ K \quad \text{and} \quad \frac{\rho_2}{\rho_{ref}} \approx 4 \times 10^{-2}\right)$, the radiation that occurred at $\lambda > 0.6\mu$ had reduced to less than 30 percent of the integrated amount between 0.2μ and 4.0μ. (See ref. 4.)

In this section of the report, the spectral radiometer data are evaluated from the standpoint of the theory contained in the aforementioned references. Because of the changing nature of the radiation during the varying conditions of reentry, each data period is analyzed separately as a unique experiment. Because severe body motions were experienced during the Fire I experiment beginning at a time late in the first data period and continuing throughout the reentry (refs. 3 and 15), a comparison of data between the two flights is restricted to the first data period.

The calorimeter experiments for the two Fire reentries are discussed in detail in references 1 and 2. The broadband radiometer data and analyses are covered in references 3 and 4. The trajectory data and atmospheric conditions for the two flights are included in references 15 and 16.

First Data Period Experiment

Experiment conditions.- The first data period experiment consisted of obtaining spectral steradiancy measurements from the stagnation flow field during the early reentry. The starting and ending conditions for the Fire I and Fire II experiments are given in the following table:

Experiment	Conditions	Elapsed time, sec	Velocity		ρ_∞/ρ_{std}
			km/sec	fps	
Fire I	Starting	1658.95	11.60	38 048	3.09×10^{-6}
	Ending	1665.90	11.53	37 848	6.79×10^{-6}
Fire II	Starting	1631.30	11.37	37 312	8.52×10^{-6}
	Ending	1636.47	11.30	37 060	8.25×10^{-5}

(The starting points for these early radiation experiments were governed by the threshold sensitivity of the radiometer. The ending condition for the Fire I experiment was determined by the onset of severe body motions.) Prior to $t_{II} = 1634$ sec, the stagnation flow field and the radiation therefrom were estimated from the theory of reference 17 to be in a wholly nonequilibrium state. After $t_{II} = 1634$ sec, the theory indicated increasing radiation from equilibrium sources. By the end of the first data period experiment, about 80 percent of the stagnation radiation at wavelengths longer than 0.2μ was estimated

to result from these equilibrium sources. On the basis of theoretical estimates, therefore, the first data period stagnation experiment spanned from a condition of wholly nonequilibrium flow to one of strong equilibrium influence. An attempt has been made to identify some of the contributing species in these Fire spectra. It is believed that these spectra are the first obtained for nonequilibrium air at conditions of early reentry.

Experimental data and theoretical comparisons.- Eight scans from the Fire II spectral radiometer record which were reduced to steradiancy units of $W/cm^2\text{-}sr\text{-}\mu$ are shown in figure 1. The scans, selected at specific times during the first data period experiment, trace out essentially a time history of the growth and intensity of the spectral distribution of radiation in the wavelength range from 0.3μ to 0.6μ. Also indicated in figure 1 are the elapsed time, scan direction, and free-stream density conditions corresponding to each spectrum. Flight velocity and the calculated shocked gas properties of temperature and density are indicated in figures 1(e) to 1(h). The nonequilibrium condition of the flow field characterized by the spectra in figures 1(a) to 1(d) preclude any determination of thermodynamic properties.

Six Fire I spectra are also shown in figure 1. They have been matched with the Fire II spectra at the same free-stream density conditions. As a result, the differences in the steradiancy levels exhibited by the two spectra may be indicative of a strong velocity dependence of radiation at these flight conditions. The higher telemetry noise levels for the Fire I experiment are noticeable. The approximately 0.01μ-wide dropout bands in the Fire I spectra (one band in fig. 1(c) and two bands in fig. 1(d)) were the result of an "excessive noise" filter built into the data reduction process. The wavelength range covered by each scan direction for each experiment is presented in the section "Instrumentation."

The following discussion of the Fire I and Fire II spectra presented in figure 1 traces the spectral time history of radiation from early reentry through the nonequilibrium phase to a condition characterized by strong equilibrium radiation.

$\frac{\rho_\infty}{\rho_{std}} = 3.0 \times 10^{-6}$.- The earliest radiation signals were indicated by the Fire I radiometer at $t_I = 1658.95$ sec. The Fire I reentry package velocity at this time was approximately 11.60 km/sec (38 048 fps) and the altitude was 89.1 km (292 400 ft). At the corresponding free-stream density conditions the Fire II radiometer did not exhibit any discernible data signals. The spikes at $\lambda \approx 0.31\mu$ and $\lambda \approx 0.53\mu$ in the Fire II spectrum were noise or otherwise spurious signals. The Fire II reentry package velocity at the time was 11.37 km/sec (37 316 fps) and the altitude was 89.1 km (293 000 ft).

The Fire I data indicated peaks at about 0.321μ and 0.348μ. These appear from the theory (e.g., refs. 7, 11, and 18) to be band heads of the $N_2^+(1\text{-})$ molecular band system. These band edges are known to occur at 0.3308μ and 0.3582μ. (See table I.)

$\frac{\rho_\infty}{\rho_{std}} = 8.0 \times 10^{-6}$.- The scan at $\frac{\rho_\infty}{\rho_{std}} = 8.0 \times 10^{-6}$ exhibited the first discernible Fire II signal at approximately 0.348μ. The entry velocity at this point was still 11.37 km/sec and the altitude was 83.8 km (275 000 ft). This signal is estimated from the theory to be the (1,0) band of the $N_2^+(1-)$ system at 0.3582μ. (See table I.) The signal at approximately 0.53μ is a noise spike. The Fire I spectrum at the corresponding free-stream density condition was completely masked by excessive telemetry noise.

$\frac{\rho_\infty}{\rho_{std}} = 1.9 \times 10^{-5}$.- The Fire II scan at $\frac{\rho_\infty}{\rho_{std}} = 1.9 \times 10^{-5}$ occurred some 2 sec after the previous one shown. The free-stream density conditions for this scan correspond to an altitude of approximately 78.6 km (258 000 ft). The velocity was still 11.37 km/sec. The Fire II scan is particularly significant in that it corresponds very closely to the entry conditions used for the preflight theoretical flow-field studies of references 13 and 14. In figure 2, the scan is compared with the estimated spectral distributions of references 13 and 14. These theories indicate only rough approximations of the spectral distribution, since the calculations were very broadband. It may be noted that there are orders of magnitude difference between the theoretical distributions and the Fire II data. The Fire II scan was chosen for comparison in figure 2 because the velocity agreed more closely with that used in the flow-field calculations.

In the Fire II scan, the $N_2^+(1-)$ band head indicated at 0.348μ has increased in intensity. Also shown are the first discernible signals at approximately 0.380μ and 0.410μ. These are assumed to be other band heads of the $N_2^+(1-)$ molecular band system. The wavelengths at which these band edges might be expected to occur (0.3914μ and 0.4278μ, respectively, table I) differ by as much as 0.0178μ from the peak intensity wavelengths indicated by the Fire data.

The corresponding Fire I spectral scan (V_I = 11.59 km/sec (38 000 fps)) indicates what is estimated to be the radiation primarily from five $N_2^+(1-)$ bands. (See table I.) The scan shows the maximum intensity points of these bands to occur at approximately 0.31μ, 0.327μ, 0.35μ, 0.38μ, and 0.41μ. These maximum intensity points correspond quite closely to the theoretical band-head locations at 0.31μ and 0.327μ but are shifted toward the low wavelength end of the spectrum at the longer wavelengths.

$\frac{\rho_\infty}{\rho_{std}} = 2.6 \times 10^{-5}$.- The molecular band radiation of the previous spectra has continued to increase in intensity. The nonequilibrium flow in the stagnation region at these times during the Fire I and Fire II reentries was estimated to correspond to the condition of incipient truncation, which was defined in reference 4 as the condition of impending radiation from equilibrium sources. The Fire I and Fire II velocities are still

essentially constant at 11.58 km/sec and 11.36 km/sec, respectively. Several new responses have appeared in the Fire I spectrum between 0.4μ and 0.6μ. The radiation intensity of these new signals are slightly in excess of 0.1 W/cm^2-sr-μ at this time. There is no indication of these responses in the Fire II scan at the same free-stream density condition.

$\frac{\rho_\infty}{\rho_{std}} = 3.7 \times 10^{-5}$.- The new signals between 0.4μ and 0.6μ in the Fire I scan have increased in intensity and are believed to result from unidentified molecular band radiation. Several $N_2^+(1-)$ bands are still indicated in both the Fire I and Fire II spectra.

$\frac{\rho_\infty}{\rho_{std}} = 4.8 \times 10^{-5}$ and $\frac{\rho_\infty}{\rho_{std}} = 5.8 \times 10^{-5}$.- Despite the noise level, the Fire I spectra at the time corresponding to $\frac{\rho_\infty}{\rho_{std}} = 4.8 \times 10^{-5}$ and 5.8×10^{-5} appear to be clearer and more consistent than the corresponding Fire II spectra. The inconsistency in the Fire II spectra is in the apparently shifting wavelength scale, however, and not in the relative intensity level. Over the range of entry conditions covered by these two and the previous two scans $\frac{\rho_\infty}{\rho_{std}} = 2.6 \times 10^{-5}$ to $\frac{\rho_\infty}{\rho_{std}} = 5.8 \times 10^{-5}$ the intensity of the spectra between 0.4μ and 0.6μ has increased more than an order of magnitude. In addition to exhibiting an increasing intensity level, the time history of radiation indicated by the Fire I spectra in the wavelength range between 0.3μ and 0.45μ during this time interval illustrates an increase in underlying continuum strength in that spectral region. The theory indicates that such an increase would be expected with increasing equilibrium radiation. The Fire I scan at $t_I = 1665.60$ sec was one of the very last prior to the onset of the violent body motions which were experienced beginning at $t_I = 1665.90$ sec in that experiment. (See refs. 3 and 15.)

$\frac{\rho_\infty}{\rho_{std}} = 8.3 \times 10^{-5}$.- The final scan at $\frac{\rho_\infty}{\rho_{std}} = 8.3 \times 10^{-5}$ of the Fire II experiment was obtained just prior to the time at which it was calculated that the surface of the exterior quartz window reached its melting point. The estimated increase in continuum radiation coupled with the possible error in reading the Fire II wavelength scale made it difficult to identify and distinguish between individual peaks in this spectrum. The increase in radiation between 0.4μ and 0.6μ produced a nearly constant-intensity spectrum between 0.3μ and 0.6μ. It was estimated from the theory (ref. 10) that the plasma radiation was dominated by line and continuum contributions. The line radiation, however, occurred mostly outside the wavelength range of the spectral radiometer. The continuum radiation was estimated to consist of contributions from the O^+ and N^+ deionization, O^- photo-detachment radiation, and electron scattering continua.

[redacted]

Second Data Period Experiment

Experiment conditions.- The second data period experiment consisted of obtaining spectral steradiancy measurements from the stagnation flow field during the early portion of exposure of the second beryllium calorimeter and prior to transmission degradation of the quartz window. The starting and ending conditions for the Fire II second data period experiment are given in the following table:

Condition	Elapsed time, sec	Altitude		Velocity		ρ_∞/ρ_{std}
		km	ft	km/sec	fps	
Starting	1642.47	54.34	178 200	10.61	34 815	5.42×10^{-4}
Ending	1642.90	53.23	174 700	10.50	34 460	6.18×10^{-4}

The data recorded by the spectral radiometer indicate the movement of the phenolic-asbestos ablation shield sufficient to block light transmission to the spectral radiometer occurred at 1642.40 sec. The next five scans of the radiometer beginning at 1642.48 sec and ending at 1642.83 sec are considered in this report (fig. 3). Heating calculations indicate some transmission degradation of the fused quartz window can be expected after this time period. The calculated values of stagnation, equilibrium temperature, and density behind the shock are given in the following table:

Scan	Elapsed time, sec	T_2, ^oK	Log ρ_2/ρ_{ref}
1	1642.48	11 140	-2.100
2	1642.57	11 122	-2.088
3	1642.66	11 106	-2.078
4	1642.75	11 088	-2.066
5	1642.83	11 071	-2.055

Experimental data and theoretical comparisons.- The radiation spectra measured during the second data period of the Fire II reentry are presented in figure 3. The five selected scans of the spectral radiometer displayed a nearly constant level of radiation from 0.3μ to 0.6μ. Superimposed on this constant level of radiation are several significant signals which are suspected to be either molecular band heads or deionization continua. The lack of repeatability of the successive scans during the second data period made it most difficult, if not impossible, to positively identify any contributing molecular radiation.

Between 0.33μ and 0.34μ on the first scan there appears a pronounced signal which is estimated to be radiation from the $N_2^+(1-)$ (2,0) bandhead at 0.3308μ. (See table I.) This molecular radiation is superimposed on strong underlying continuum radiation which

[redacted]

is believed to consist primarily of N^+ and O^+ deionization and O^- photodetachment radiation. At these flight conditions, this continuum radiation is predicted to be dominant. This signal at 0.3308μ appears to have rapidly diminished in intensity or shifted its position on succeeding scans.

In figure 4, theoretical spectral distributions are compared with the experimental Fire spectra. The experimental scan at $t_{II} = 1642.66$ sec was selected for comparison because the flight conditions of velocity and free-stream density corresponded more closely with those of the theoretical predictions of references 12 and 13. Also shown in figure 4 is a theoretical estimate based on the more recent values of absorption coefficients of air given in reference 19. Radiation cooling was estimated in reference 20 to reduce theoretical estimates of radiation in the $\lambda > 0.2\mu$ wavelength range by a factor of 0.7. This effect has been applied to the theory of reference 19 in figure 4. The agreement between the flight data and the theory of reference 19 (adjusted for cooling by ref. 20) is reasonably good. The decrease in spectral intensity at wavelengths longer than 0.45μ indicated by the flow-field studies (refs. 12 and 13) is not supported by the Fire data.

Third Data Period Experiment

Experiment conditions.- The third data period of the Fire II reentry began with the exposure of a cool radiometer window at approximately $t_{II} = 1648.16$ sec. Although the total radiometer data (ref. 4) exhibited some erratic behavior after $t_{II} = 1648.50$ sec, radiometer window heating calculations indicate that the condition of surface melting of the outer quartz window for the third data period occurred at $t_{II} = 1648.84$ sec. Therefore the measurements of the spectral steradiancy in the stagnation flow field are considered to be valid to $t_{II} = 1648.84$ sec. The starting and ending flight conditions for this experiment period were as follows:

Conditions	Elapsed time, sec	Altitude		Velocity		ρ_∞/ρ_{std}
		km	ft	km/sec	fps	
Starting	1648.16	41.80	137 100	8.20	26 910	2.54×10^{-3}
Ending	1648.84	40.57	133 100	7.74	25 410	3.04×10^{-3}

Since the third data period was timed to occur on the back side of the heat pulse, it was characterized by equilibrium radiation at relatively low velocities and decreasing gas-cap temperatures. The stagnation-point radiation occurred at calculated gas-cap temperatures ranging from $T_2 = 7845^\circ$ K to 7597° K and density ratios ranging from $\frac{\rho_\infty}{\rho_{ref}} = 10^{-1.413}$ to $10^{-1.351}$.

[redacted]

Experimental data.- The radiation spectra measured during the third data period of the Fire II reentry are presented in figure 5. Each of the eight spectral scans is identified by the elapsed time, scan direction, and the calculated equilibrium temperature and density ratio for the gas cap behind the shock.

Although the reentry environment for both the second and third data periods was characterized by radiation at equilibrium conditions, the spectra obtained during the two periods were significantly different. The dominance of molecular band system radiation at the lower gas-cap temperatures of the third data period is clearly indicated by the prominent peaks in the spectra of figure 5.

An assessment of the inaccuracy associated with wavelength determination can be readily obtained from the spectra. Since the radiation spectrum of a neutral or ionized molecule is known to be unique, the wavelength positions of the prominent molecular band heads are known and should remain fixed from scan to scan. Overlay comparisons of the spectra of figure 5 indicate that during the elapsed time of the third data period (0.68 sec) the positions of the prominent peaks shown in the four forward scans shifted progressively toward the red by a total of approximately 0.008μ. The peaks shown in the third and fourth backward scans (figs. 5(e) and 5(g)) were displaced toward the violet (by approximately 0.010μ and 0.006μ, respectively) with respect to those shown for the first scan (fig. 5(a)). Thus the wavelength location of any given peak could be in error by as much as 0.01μ.

All of the prominent peaks shown in the spectra of figure 5 are attributed primarily to radiation from the $N_2^+(1-)$ band system. The wavelengths of the stronger band heads and the associated upper and lower state vibration quantum numbers of the $N_2^+(1-)$ system (taken from ref. 18) are presented in table I. The major peaks in the third data period spectra are identified by their vibration quantum numbers shown on the spectrum of figure 5(d). All of the strongest bands of the $N_2^+(1-)$ system are known to be degraded (shaded) toward the violet (see, for example, ref. 21) with the sharp band edges on the long wavelength side of the prominent peaks. This degradation and the associated band edges can be recognized in the spectra of figure 5 in most instances. Thus it appears that the resolution of the spectral radiometer was sufficient to allow positive identification of the major radiating species $N_2^+(1-)$ as well as other individual bands.

Comparison with theory.- Figure 6 shows a comparison of a measured radiation spectrum with that predicted by the use of the theories of references 7 and 19. The theoretical spectrum for a density ratio of $\frac{\rho_\infty}{\rho_{ref}} = 10^{-1.4}$ was obtained by an interpolation between those presented in reference 7 for density ratios of $\frac{\rho_\infty}{\rho_{ref}} = 10^{-2}$ and $\frac{\rho_\infty}{\rho_{ref}} = 10^{-1}$ and a gas temperature $T_2 = 8000^\circ$ K. Reference 7 was chosen for

[redacted]

comparison because, as reported in reference 4, it appeared to provide the best agreement between the measured and predicted values of the total radiation (integrated over the entire spectrum) during the third data period when molecular band radiation was dominant. Reference 7 uses the Mayer-Goody model for an electronic-vibrational band. This model supposes a statistical distribution of spectral lines in any particular region of the spectrum. The further assumption that the halfwidths of the spectral lines are very large leads to an effectively continuous distribution of radiation within the confines of the electronic-vibrational band. The constants used in reference 7 for the $N_2^+(1-)$ system were taken from reference 21. An experimental value of the electronic oscillator strength equal to 0.04 was used. Considering the experimental inaccuracies involved in the measured spectra, the theory of reference 7 appears to provide a very good prediction of both the magnitude and shape of the air radiation spectrum in the wavelength region from 0.3μ to 0.6μ and at gas-cap temperatures around 8000° K. The theory of reference 19, also shown in figure 6, is not in quite as good agreement with the Fire data at this flight condition.

CONCLUSIONS

The Project Fire experiments have provided measurements of the intensity and spectral distribution of radiation experienced by a blunt body entering the earth atmosphere at lunar return velocities. These spectra, which cover a nominal wavelength range between 0.2μ and 0.6μ, were obtained in a clean (uncontaminated) environment at the stagnation region. The experimental results indicate the following conclusions:

1. During the very early reentry, where nonequilibrium conditions are expected to prevail in the forebody flow field of the Fire reentry package, the radiation from the plasma in the stagnation region was dominated by contributions from the $N_2^+(1-)$ molecular band system. The data indicated that the underlying radiation, initially quite low during this period, increased in intensity with increasing time. The results of the nonequilibrium radiation measurements were orders of magnitude smaller than preflight predictions.

2. At the peak heating conditions, the radiation was dominated by a nearly constant intensity distribution over the 0.3μ to 0.6μ wavelength range. Certain theoretical estimates of the radiation levels at these flight conditions were in reasonably good agreement with the experimental results.

3. At the conditions of decreasing radiation on the trailing side of the heat pulse, the spectral distributions were again dominated by the contributions from the $N_2^+(1-)$ molecular band system. The experimental intensity levels corroborated very well the theoretical predictions at these conditions.

Langley Research Center,
National Aeronautics and Space Administration,
Langley Station, Hampton, Va., May 1, 1967,
714-00-00-01-23.

APPENDIX A

SUPPLEMENTAL DATA

In addition to those selected for presentation in this paper, there exist many additional spectra obtained during the Fire I and Fire II reentries. Although most of these spectra were obtained outside the prime data periods, there are available additional spectra obtained during the first data period of each Fire experiment. A complete record of all the spectra obtained during the Fire I and Fire II reentries is available in the form of two 35-mm film-strip supplements (film serial L-961, Parts I and II). The data in the film strips appear as plots of radiation intensity in W/cm^2-sr-μ against wavelength in Å. These supplements may be obtained on loan by the use of the request form contained in this report. The film strips can be used to provide enlarged projections of the spectra.

Each spectrum on the film is identified with the instrument scan direction and the elapsed time from launch. The flight conditions (altitude, velocity, and free-stream density) and thermodynamic conditions in the shocked gas (temperature and density) for both the Fire I and Fire II experiments are tabulated as a function of elapsed time in table I of references 3 and 4, respectively. Additional information applicable to the Fire II experiment which may be useful to the reader can be found in references 4 and 22. Reference 4 (appendix C) discusses the radiometer data obtained outside the prime data periods, whereas reference 22 provides a time history of the ground-based photographic and spectrographic coverage in the reentry area.

It should be noted that the usefulness of the supplementary spectra obtained outside the prime data periods as defined in this report is probably very limited. The limitations are due to deterioration of the radiometer windows; flow-field contamination by ablation products while phenolic-asbestos heat shields are exposed; and, for the Fire I spectra, by the large body motions which terminated the first data period and prevailed throughout the remainder of the experiment. These Fire I spectra were recorded during large angle-of-attack variations of the body and thus the wavelength scans are not entirely representative of stagnation conditions.

REFERENCES

1. Cornette, Elden S.: Forebody Temperatures and Total Heating Rates Measured During Project Fire 1 Reentry at 38 000 Feet Per Second. NASA TM X-1120, 1965.
2. Cornette, Elden S.: Forebody Temperatures and Calorimeter Heating Rates Measured During Project Fire II Reentry at 11.35 Kilometers Per Second. NASA TM X-1305, 1966.
3. Cauchon, Dona L.: Project Fire Flight 1 Radiative Heating Experiment. NASA TM X-1222, 1966.
4. Cauchon, Dona L.: Radiative Heating Results From the Fire II Flight Experiment at a Reentry Velocity of 11.4 Kilometers Per Second. NASA TM X-1402, 1967.
5. Kivel, B.; and Bailey, K.: Tables of Radiation From High Temperature Air. Res. Rept. 21 (Contracts AF 04(645)-18 and AF 49(638)-61), AVCO Res. Lab., Dec. 1957.
6. Meyerott, R. E.; Sokoloff, J.; and Nicholls, R. W.: Absorption Coefficients of Air. GRD-TR-60-277 (Geophys. Res. Papers No. 68), U.S. Air Force, July 1960.
7. Breene, R. G., Jr.; and Nardone, Maria: Radiant Emission From High Temperature Equilibrium Air. R61SD020 (Contract No. AF04(647)-269), Space Sci. Lab., Gen. Elec. Co., May 1961.
8. Richardson, Norman R.: Project Fire Instrumentation for Radiative Heating and Related Measurements. NASA TN D-3646, 1966.
9. Nardone, M. C.; Breene, R. G.; Zeldin, S. S.; and Riethof, T. R.: Radiance of Species in High Temperature Air. Tech. Inform. Ser. R63SD3 (Contract AF 04(694)-222), Missile and Space Div., Gen. Elec. Co., June 1963. (Available from DDC as AD No. 408564.)
10. Allen, Richard A.: Air Radiation Graphs: Spectrally Integrated Fluxes Including Line Contributions and Self Absorption. Res. Rept. 230 (Contract Nos. NASw-748 and DA-01-021-AMC-12005(Z)), Avco-Everett Res. Lab., Sept. 1965.
11. Allen, Richard A.: Air Radiation Tables: Spectral Distribution Functions for Molecular Band Systems. Res. Rept. 236 (Contracts NASw-748 and DA-01-021-AMC-12005(Z)), Avco-Everett Res. Lab., Apr. 1966.
12. Brunner, M. J.; Dohner, C. V.; Langelo, V. A.; and Rie, H.: Flow Field Prediction and Analysis – Project Fire. Doc. No. 64SD727 (NASA CR-60451), Re-Entry Syst. Dept., Gen. Elec. Co., May 29, 1964.

13. Vinokur, M.; Nicolet, W. E.; Buckingham, A. C.; and Hoshizaki, H.: Project Fire – Flow Field Prediction and Analysis. M-12-65-1 (NASA CR-63401) Lockheed Missiles & Space Co., Mar. 1965.

14. Kuby, W. C.; Byron, S. R.; Foster, R. M.; Hoglund, R. F.; and Holt, M.: Analysis of the Project Fire Re-Entry Package Flow Field. Publ. No. U-3020 (NASA CR-63388), Aeronutronic Div., Philco Corp., Oct. 8, 1964.

15. Scallion, William I.; and Lewis, John H., Jr.: Flight Parameters and Vehicle Performance for Project Fire Flight 1, Launched April 14, 1964. NASA TN D-2996, 1965.

16. Lewis, John H., Jr.; and Scallion, William I.: Flight Parameters and Vehicle Performance for Project Fire Flight II, Launched May 22, 1965. NASA TN D-3569, 1966.

17. Allen, R. A.; Rose, P. H.; and Camm, J. C.: Nonequilibrium and Equilibrium Radiation at Super-Satellite Re-Entry Velocities. Res. Rept. 156 (BSD-TDR-62-349), Avco-Everett Res. Lab., Sept. 1962.

18. Pearse, R. W. B.; and Gaydon, A. G.: The Identification of Molecular Spectra. Third ed., John Wiley & Sons, Inc., 1963.

19. Churchill, D. R.; Armstrong, B. H.; Johnston, R. R.; and Müller, K. G.: Absorption Coefficients of Heated Air: A Tabulation to 24 000° K. J. Quant. Spectry. Radiative Transfer, vol. 6, no. 4, July-Aug. 1966, pp. 371-442.

20. Olstad, Walter B.: Prediction of the Stagnation-Point Radiation Heat Transfer for the Project Fire Reentry Vehicle. NASA TM X-1401, 1967.

21. Herzberg, Gerhard: Molecular Spectra and Molecular Structure. I.- Spectra of Diatomic Molecules. Second ed., D. Van Nostrand Co., Inc., c.1950.

22. McKee, Charles W.: Project Fire Photographic Summary and Record of Reentry Phenomena at Hyperbolic Velocities. NASA TN D-3571, 1966.

TABLE I.- WAVELENGTH LOCATION OF SOME OF THE STRONGER BAND HEADS OF THE N_2^+ (1-) SYSTEM *

Wavelength, microns	Upper state vibration quantum number	Lower state vibration quantum number
0.3079	3	0
.3308	2	0
.3564	2	1
.3582	1	0
.3884	1	1
.3914	0	0
.4237	1	2
.4278	0	1
.4600	2	4
.4652	1	3
.4709	0	2
.5149	1	4
.5228	0	3
.5653	2	6
.5865	0	4

*Wavelength obtained from reference 18.

Fire I

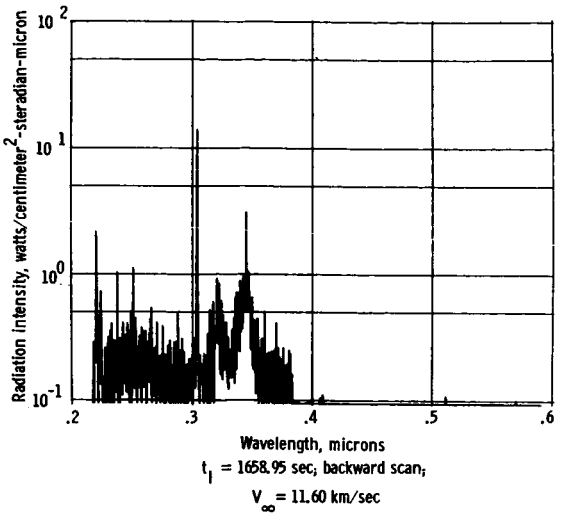

t_I = 1658.95 sec; backward scan;
V_∞ = 11.60 km/sec

Fire II

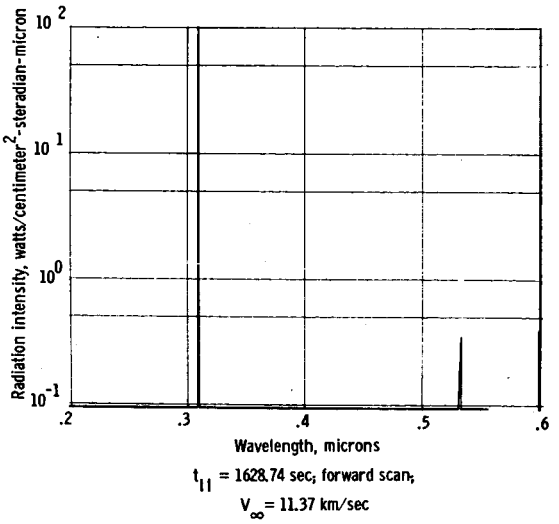

t_{II} = 1628.74 sec; forward scan;
V_∞ = 11.37 km/sec

(a) $\rho_\infty/\rho_{std} = 3.0 \times 10^{-6}$.

No data
Excessive noise

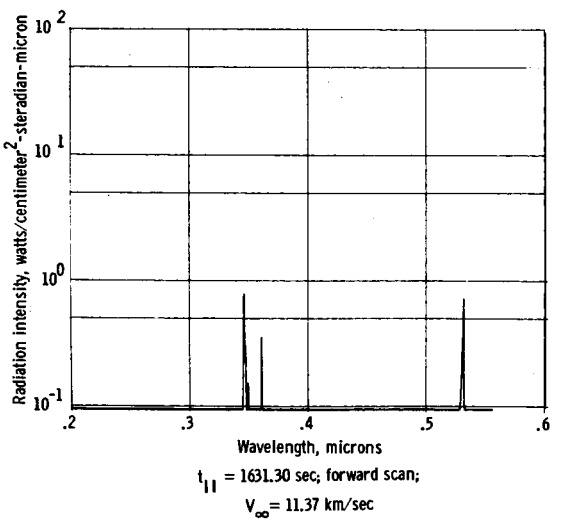

t_{II} = 1631.30 sec; forward scan;
V_∞ = 11.37 km/sec

(b) $\rho_\infty/\rho_{std} = 8.0 \times 10^{-6}$.

Figure 1.- Spectral radiometer scans obtained during first data periods of Fire I and Fire II experiments.

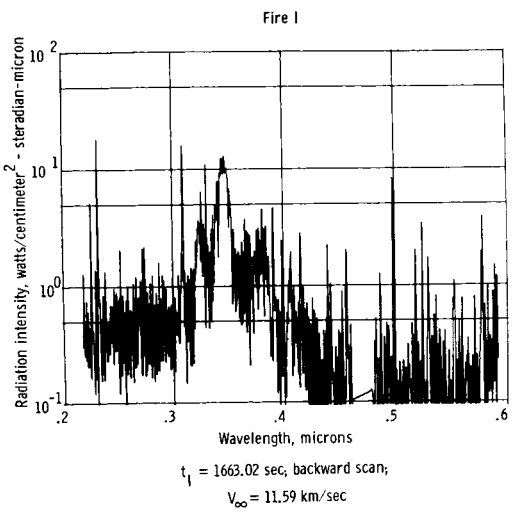

t_I = 1663.02 sec; backward scan;
V_∞ = 11.59 km/sec

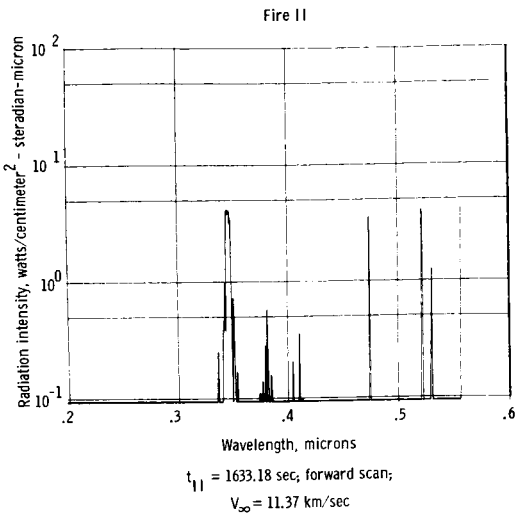

t_{II} = 1633.18 sec; forward scan;
V_∞ = 11.37 km/sec

(c) $\rho_\infty/\rho_{std} = 1.9 \times 10^{-5}$.

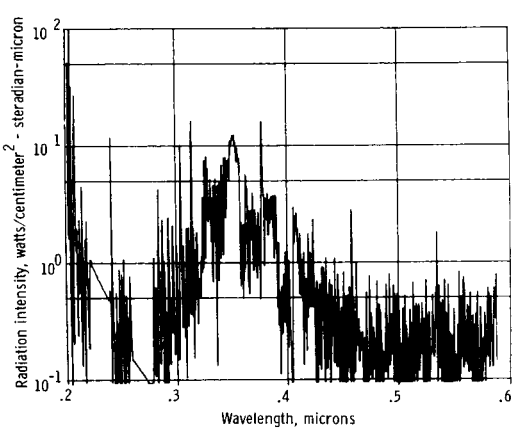

t_I = 1663.56 sec; forward scan;
V_∞ = 11.58 km/sec

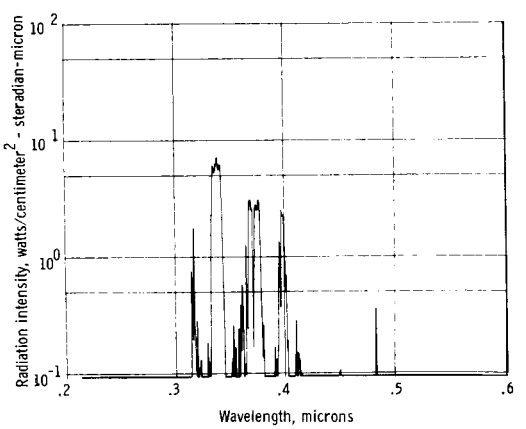

t_{II} = 1633.77 sec; backward scan;
V_∞ = 11.36 km/sec

(d) $\rho_\infty/\rho_{std} = 2.6 \times 10^{-5}$.

Figure 1.- Continued.

Fire I

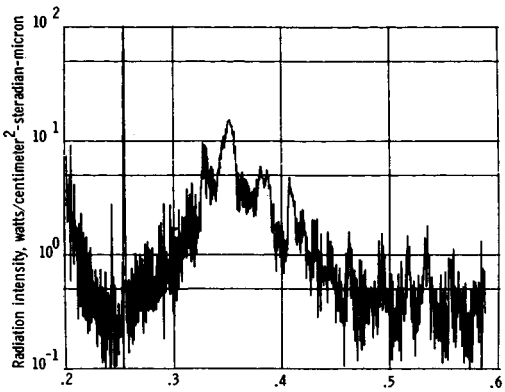

t_I = 1664.42 sec; forward scan; T_2 = 10 700° K; log ρ_2/ρ_{ref} = -3.217; V_∞ = 11.56 km/sec

Fire II

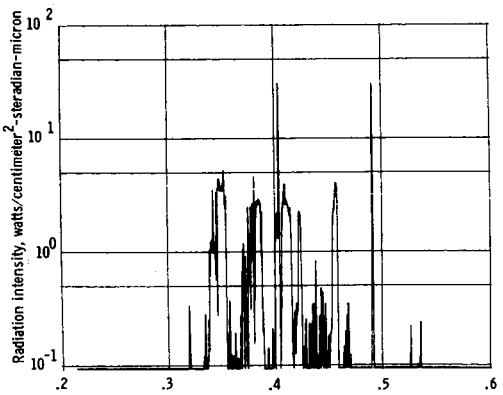

t_{II} = 1634.43 sec; backward scan; T_2 = 10 550° K; log ρ_2/ρ_{ref} = -3.215; V_∞ = 11.35 km/sec

(e) $\rho_\infty/\rho_{std} = 3.7 \times 10^{-5}$.

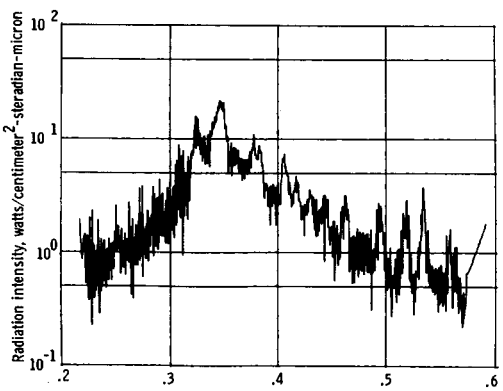

t_I = 1665.17 sec; backward scan; T_2 = 10 880° K; log ρ_2/ρ_{ref} = -3.095; V_∞ = 11.55 km/sec

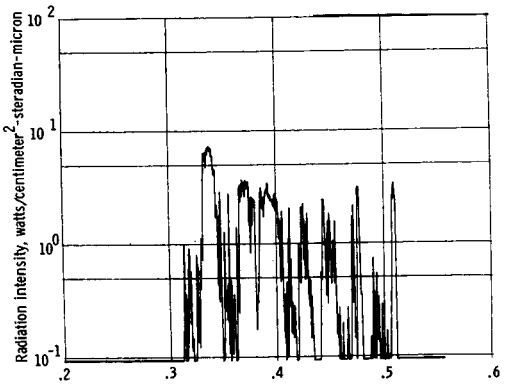

t_{II} = 1634.86 sec; forward scan; T_2 = 10 660° K; log ρ_2/ρ_{ref} = -3.130; V_∞ = 11.34 km/sec

(f) $\rho_\infty/\rho_{std} = 4.8 \times 10^{-5}$.

Figure 1.- Continued.

Fire I

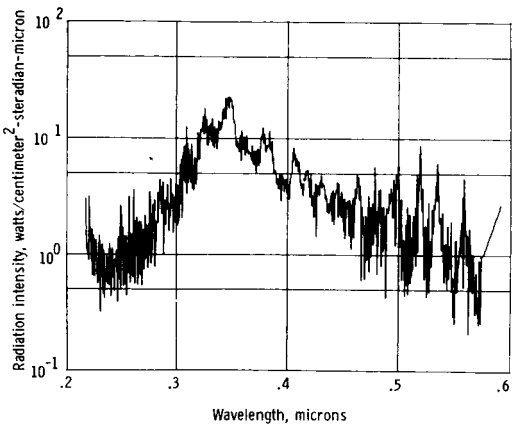

t_I = 1665.60 sec; backward scan; T_2 = 11 000° K; $\log \rho_2/\rho_{ref}$ = -3.025; V_∞ = 11.54 km/sec

Fire II

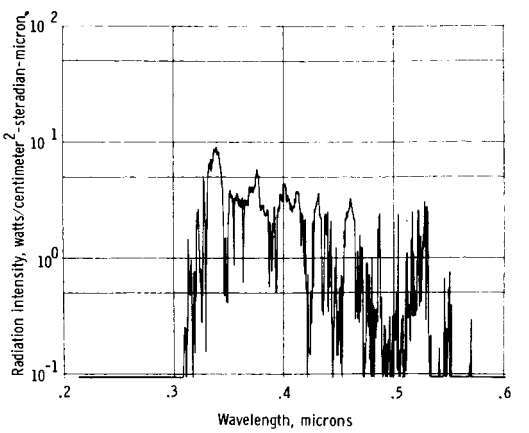

t_{II} = 1635.43 sec; backward scan; T_2 = 10 790° K; $\log \rho_2/\rho_{ref}$ = -3.037; V_∞ = 11.33 km/sec

(g) $\rho_\infty/\rho_{std} = 5.8 \times 10^{-5}$.

No data

Body motions

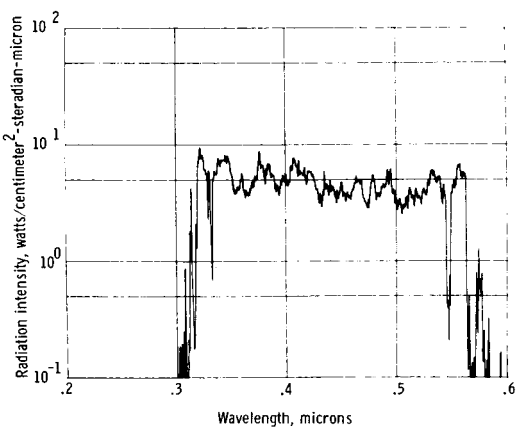

t_{II} = 1636.43 sec; backward scan; T_2 = 10 990° K; $\log \rho_2/\rho_{ref}$ = -2.884; V_∞ = 11.30 km/sec

(h) $\rho_\infty/\rho_{std} = 8.3 \times 10^{-5}$.

Figure 1.- Concluded.

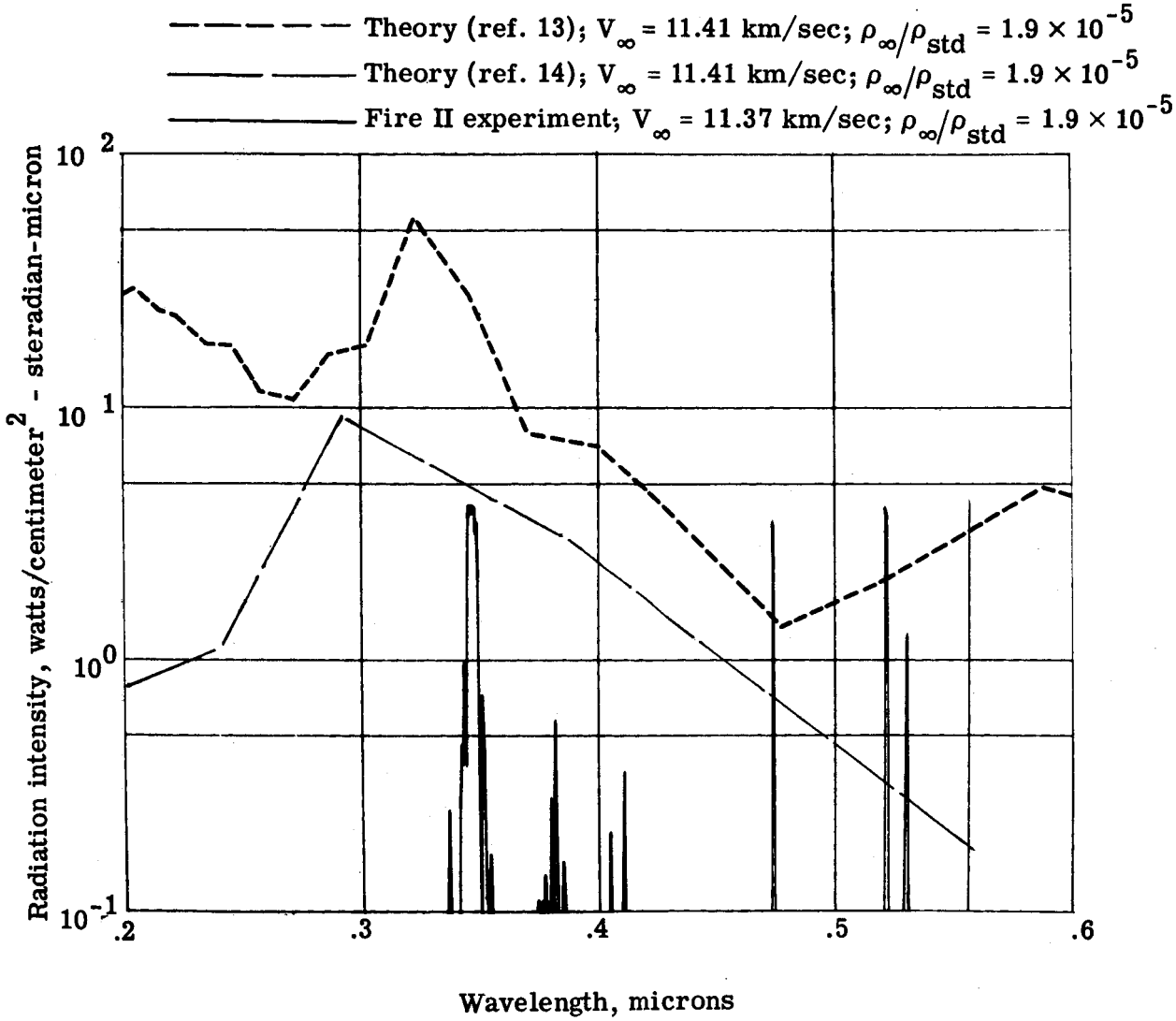

Figure 2.- Comparison of measured and predicted spectral distribution of nonequilibrium radiation for first data period of Fire II reentry.

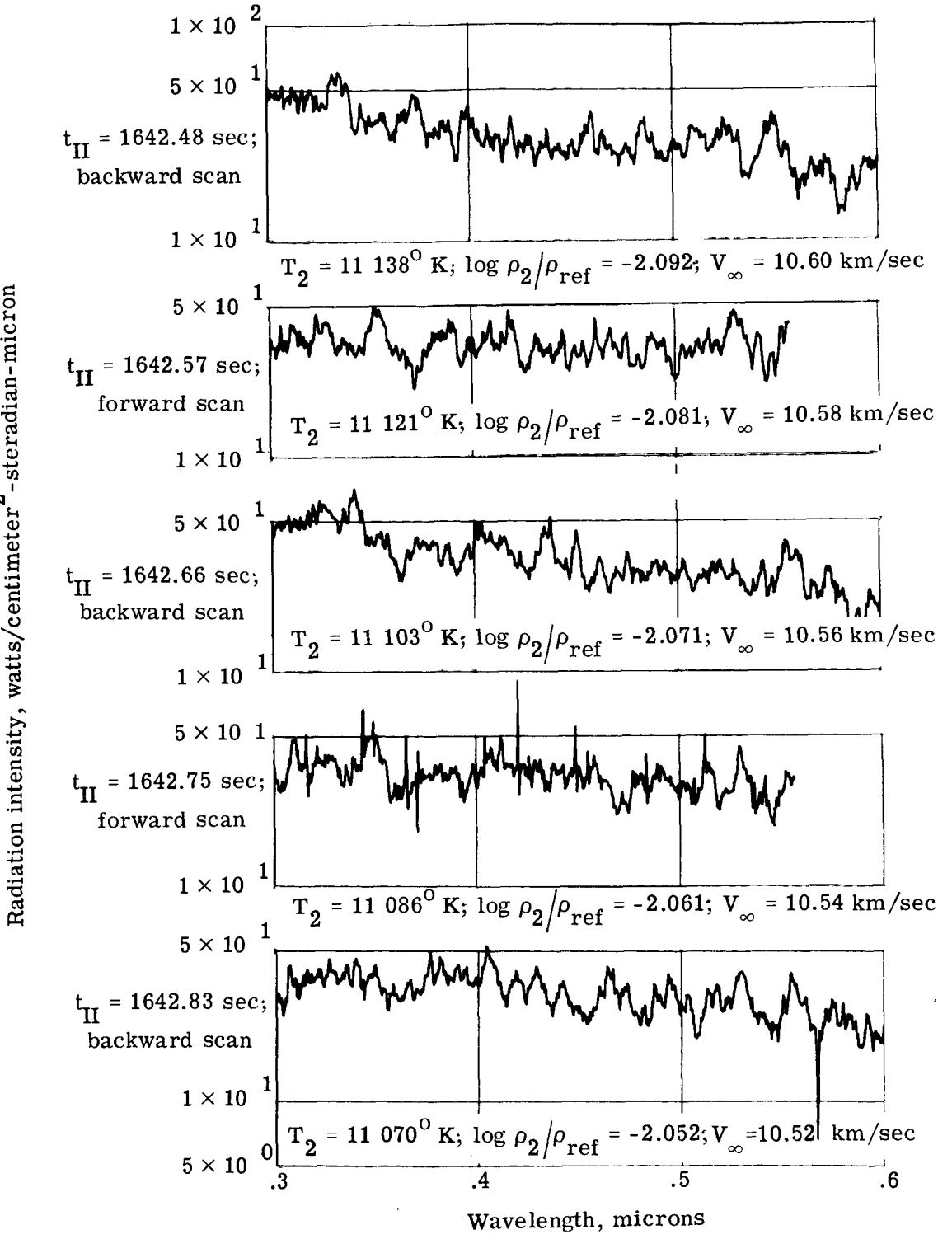

Figure 3.- Spectral radiometer scans obtained during second data period of Fire II experiment.

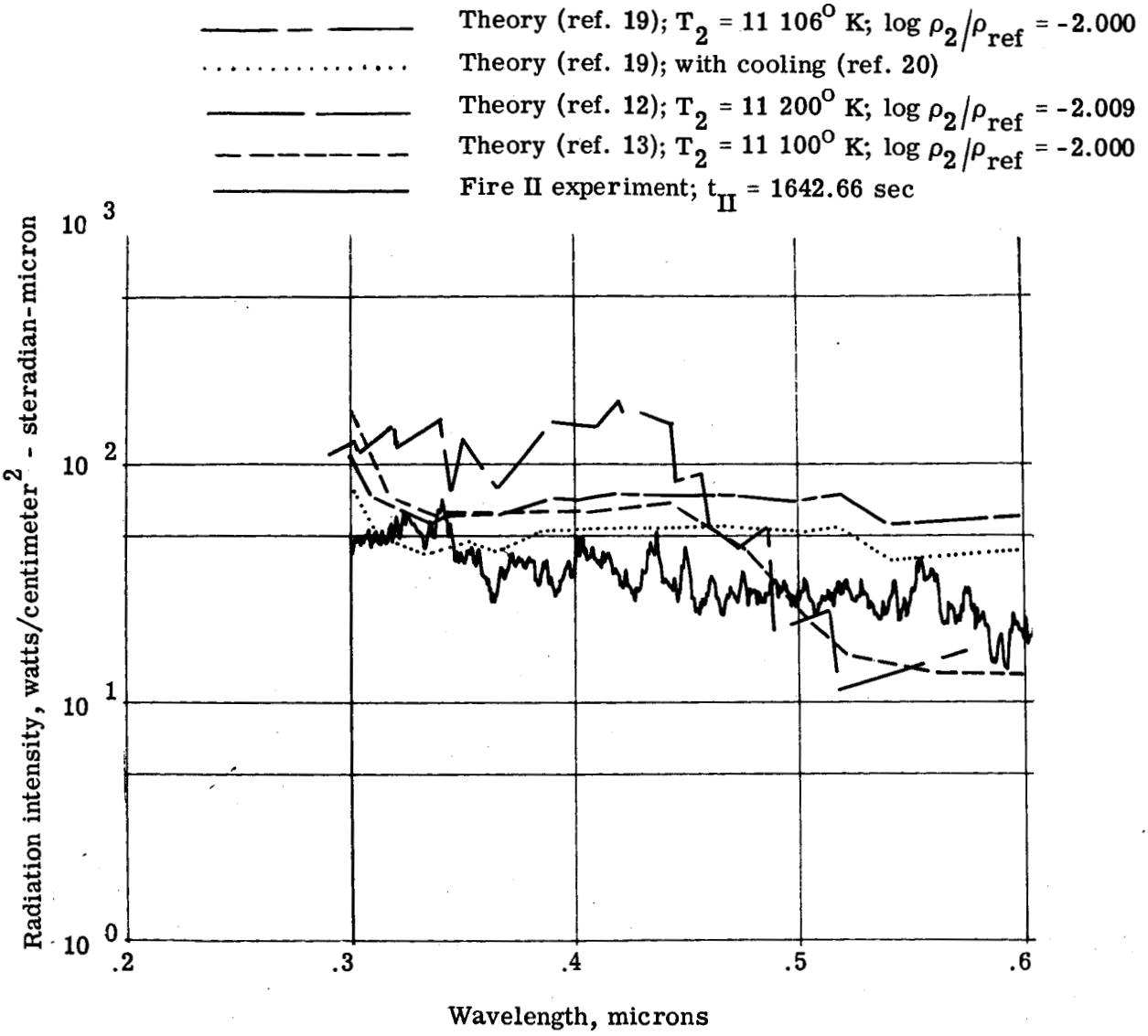

Figure 4.- Comparison of measured and predicted radiation spectra for second data period of Fire II reentry.

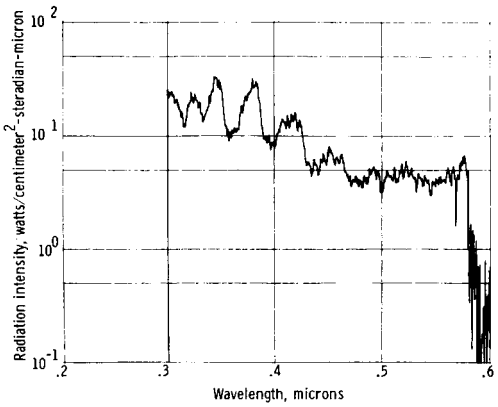

(a) t_{11} = 1648.19 sec; backward scan; $T_2 = 7845^0$ K; $\log \rho_2/\rho_{ref} = -1.413$; $V_\infty = 8.17$ km/sec.

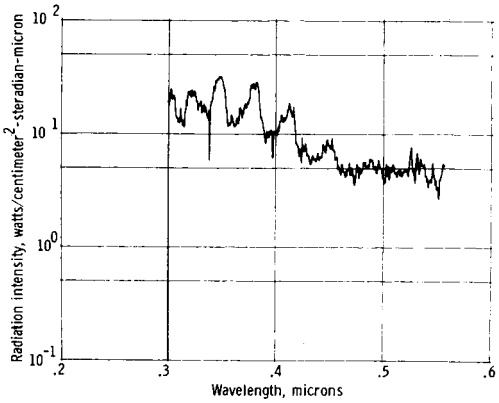

(b) t_{11} = 1648.28 sec; forward scan; $T_2 = 7808^0$ K; $\log \rho_2/\rho_{ref} = -1.404$; $V_\infty = 8.11$ km/sec.

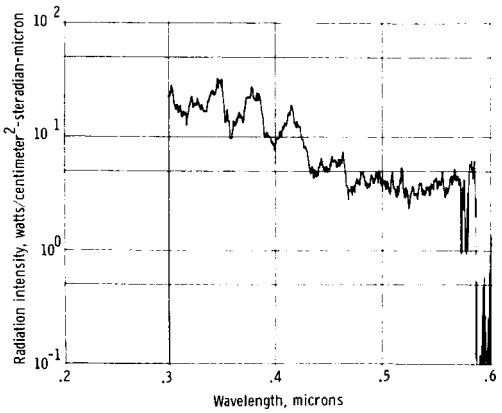

(c) t_{11} = 1648.36 sec; backward scan; $T_2 = 7775^0$ K; $\log \rho_2/\rho_{ref} = -1.395$; $V_\infty = 8.60$ km/sec.

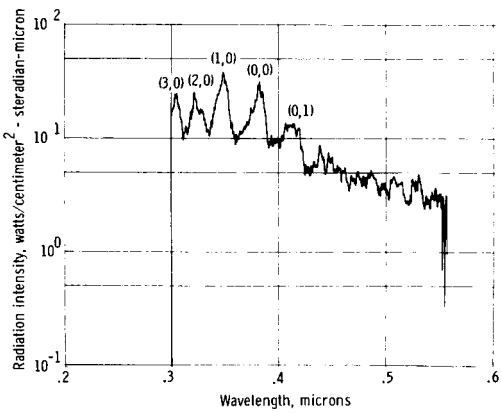

(d) t_{11} = 1648.45 sec; forward scan; $T_2 = 7738^0$ K; $\log \rho_2/\rho_{ref} = -1.386$; $V_\infty = 8.00$ km/sec.

Figure 5.- Radiation spectra obtained during third data period of Fire II reentry.

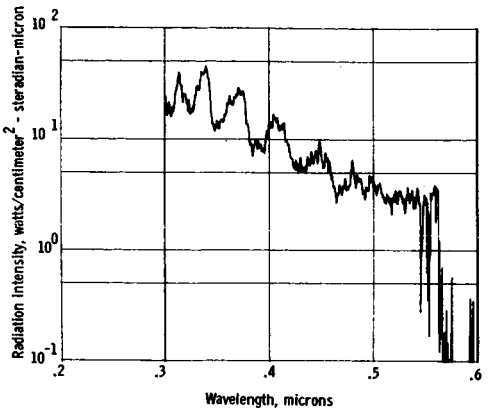

(e) t_{11} = 1648.54 sec; backward scan; $T_2 = 7702^0$ K; $\log \rho_2/\rho_{ref} = -1.376$; $V_\infty = 7.94$ km/sec.

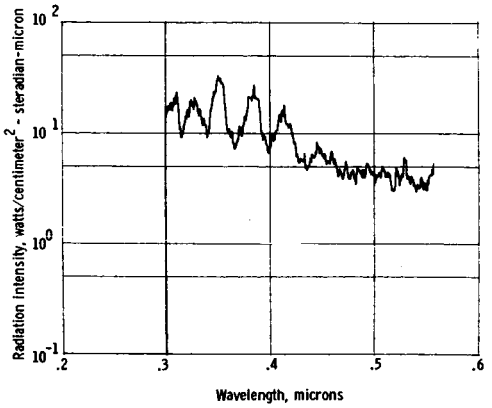

(f) t_{11} = 1648.63 sec; forward scan; $T_2 = 7665^0$ K; $\log \rho_2/\rho_{ref} = -1.367$; $V_\infty = 7.88$ km/sec.

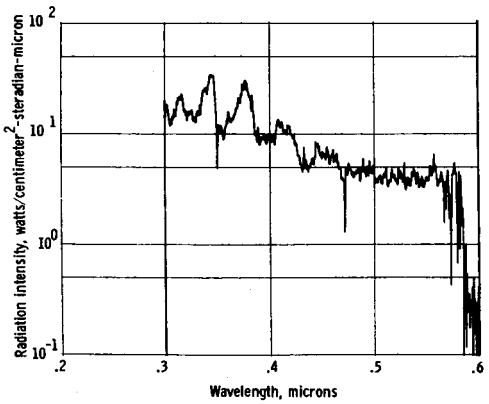

(g) t_{11} = 1648.71 sec; backward scan; $T_2 = 7630^0$ K; $\log \rho_2/\rho_{ref} = -1.359$; $V_\infty = 7.82$ km/sec.

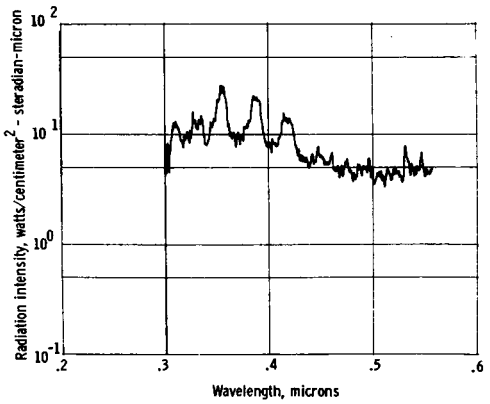

(h) t_{11} = 1648.80 sec; forward scan; $T_2 = 7595^0$ K; $\log \rho_2/\rho_{ref} = -1.351$; $V_\infty = 7.76$ km/sec.

Figure 5.- Concluded.

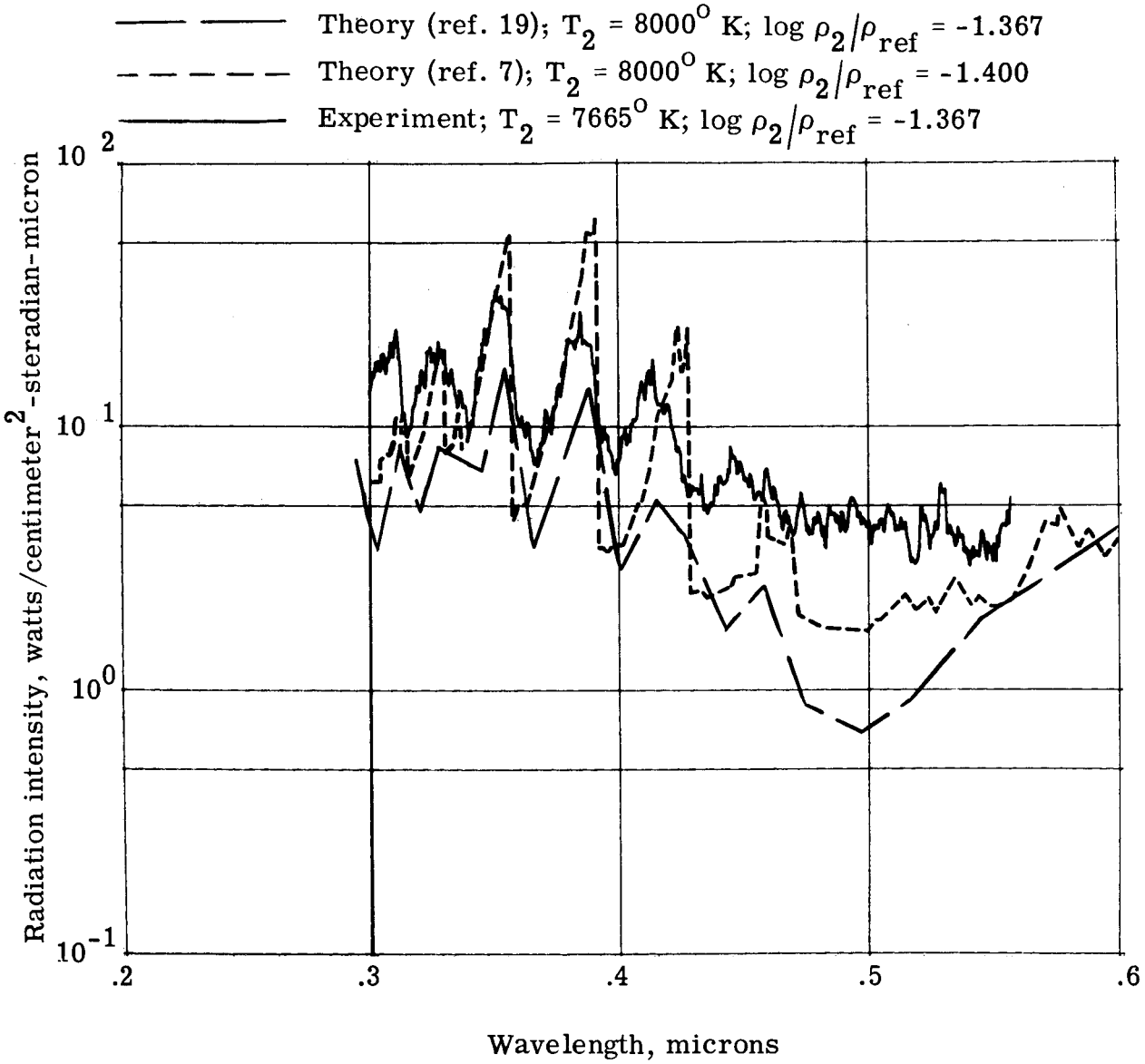

Figure 6.- Comparison of measured and predicted radiation spectra for third data period of Fire II reentry.

NASA-Langley, 1967 — 31 L-5334

[redacted]

Two film-strip supplements L-961, Parts I and II, and carrying the same classification as the report, are available on loan. Requests will be filled in the order received. You will be notified of the approximate date scheduled.

The film strips (35 mm, black and white) show the reproduced spectral radiometer scans recorded during the Fire I and Fire II reentry experiments. The data appear as plots of radiation intensity in watts per centimeter^2-steradian-micron against wavelength in angstroms.

Requests for the film should be addressed to:

Scientific and Technical Information Division
Code ATSS
National Aeronautics and Space Administration
Washington, D.C. 20546

NOTE: The handling of requests for this classified film will be expedited if application for the loan is made by the individual to whom this copy of the report was issued. In line with established policy, classified material is sent only to previously designated individuals. Your cooperation in this regard will be appreciated.

[redacted]

CUT

Date _____

Please send, on loan, copy of film-strip supplement L-961, Pts. I and II, to TM X-1389.

_____
Name of organization

_____
Street number

_____
City and State Zip code

Attention*: Mr. _____

Title _____

*To whom copy of the TM was issued

Place
Stamp
Here

Scientific and Technical Information Division
Code ATSS
National Aeronautics and Space Administration
Washington, D.C. 20546